Chemical component mapping of pulverized toner by scanning transmission X-ray microscopy

Noriyuki Iwata[a,b], Katsuhiko Tani[a], Atsuyuki Watada[a], Hiromi Ikeura-Sekiguchi[c],
Toru Araki[d], Adam P. Hitchcock[d,*]

[a]*Ricoh Co Ltd, 16-1 Shinnei-cho, Tsuzuki-ku, Yokohama 224-0035, Japan*
[b]*Graduate School for Science, Chiba University, 1-33 Yayoi-cho, Inage-ku, Chiba 263-8522, Japan*
[c]*Research Institute of Instrumentation Frontier, AIST, Tsukuba, Ibaraki 305-8568, Japan*
[d]*Brockhouse Institute for Materials Research, McMaster University, Hamilton, ON, Canada L8S 4M1*

Abstract

Toners are micron scale polymer particles constructed of several kinds of resin, pigment, wax, etc. Transmission electron microscopy (TEM) is used for observation of the dispersion of the component materials in toners, but TEM images cannot identify simultaneously all components. Scanning transmission X-ray microscopy (STXM) not only provides simultaneous observation of spatial distributions of wax, resin and carbon black in toners, but it also provides detailed, quantitative, chemical information about the wax and resin environments through chemical component maps derived from multiple energy image sequences. The capabilities of STXM for toner analysis are illustrated by results of a study of a toner for black/white copy/print applications.
© 2005 Published by Elsevier Ltd.

1. Introduction

Toners for copy machines, printers, etc. are constructed of several kinds of resin, pigment, wax and other components. The quality of a toner, with respect to fixing on paper, charging, color and gloss, is closely related to the dispersion of these components in toner. Transmission electron microscopy (TEM) has been used to study the dispersion of components in toners (Kiatkamjomwong et al., 2003; Itoh and Kishida, 2003), but, without extensive selective staining of the specimen, TEM imaging cannot easily distinguish various kinds of materials in toner particles. While electron energy loss spectroscopy in TEM or scanning transmission electron microscopy has the potential to provide chemical analysis, for most organic materials, particularly samples with aliphatic substances such as waxes, spectra of adequate quality for the desired

analysis cannot be obtained before radiation damage grossly modifies the chemistry of the sample. Scanning transmission X-ray microscopy (STXM) (Ade, 1998; Hitchcock, 2001; Ade and Urquhart, 2002) is a relatively new, synchrotron-based analytical microscopy which achieves strong chemical sensitivity through near edge X-ray absorption spectral (NEXAFS) contrast (Stöhr, 1991). In the implementation at the 5.3.2 bending magnet beamline (Warwick et al., 2002) at the Advanced Light Source (ALS) used in this work, STXM provides excellent spectroscopy in the soft X-ray regions (more than 3000 resolving power, with a photon energy range from 200 to 1200 eV), better than 40 nm spatial resolution, and the ability to maintain that spatial resolution over the full range of accessible photon energies (and thus, zone plate—sample focal distances, which must be changed linearly with energy) through the use of differential laser interferometry (Kilcoyne et al., 2003). STXM is a powerful tool for studies of polymer materials because it has strong, chemically specific contrast that is based on the intrinsic spectral properties of the components. Here, we show how the C 1s near edge X-ray absorption fine structure (NEXAFS)
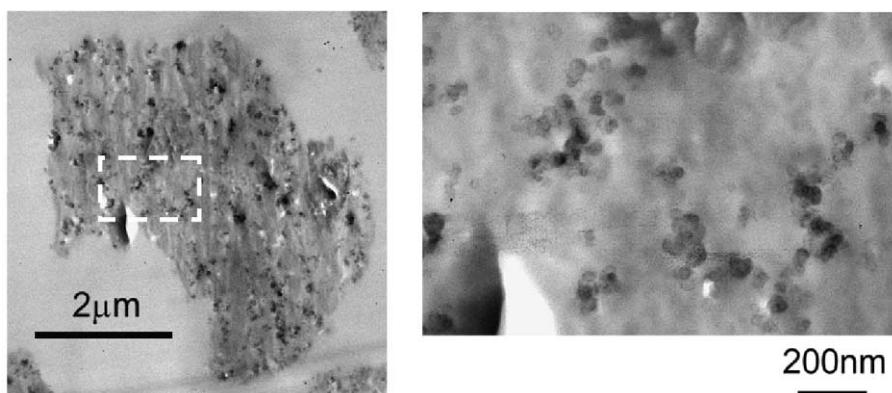

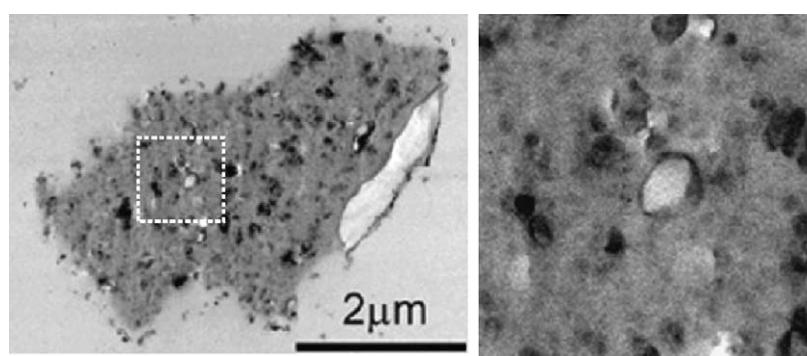Fig. 1. TEM image of unstained pulverized toner.

Fig. 2. TEM image of pulverized toner stained with RuO$_4$ vapor.

contrast of toner components, as measured in STXM, can be used for effective and quantitative chemical component mapping. Three-dimensional chemical component mapping of pulverized toner, based on reconstruction of image sequences recorded from serially microtomed sections, has been reported previously by us (Hitchcock et al., 2003). The aim of this study is to discriminate various materials in toner by STXM and to show the advantages of STXM relative to TEM.

2. Experimental

The sample was a typical pulverized toner that involved resin, wax and carbon black as the main components. The pulverized toner particles were embedded in an epoxy resin, sliced into ∼80 nm thick sections by ultra-microtomy, and placed directly on a copper grid mesh. Measurements of reference spectra of carbon black, wax and observation of the section of the toner were carried out by an interferometrically-controlled STXM (Kilcoyne et al., 2003) at beam line 5.3.2 (Warwick et al., 2002) at the ALS. The measurements were performed with the sample in a helium atmosphere. The vertical and horizontal scanning step size was 50 nm, with 2 ms dwell time per pixel. An image sequence (sometimes called a 'stack') measurement was used for detailed mapping. The energy step was 0.3 eV from

282.0 to 284.2 eV, 0.1 eV from 284.3 to 286.0 eV and 0.4 eV from 286.2 to 292 eV. Images on the sample and in a hole (I$_0$ signal) were measured alternately at each energy step. Chemical component maps were derived from image sequences by using singular value decomposition (SVD) analysis (Koprinarov et al., 2002, Hitchcock et al., 2005), implemented in the 'aXis2000' program.[1] TEM measurements were performed with a JEOL 2010 TEM at 100 kV. Unstained sections and sections stained by 5% RuO$_4$ vapor were used for TEM observations.

3. Results and discussion

3.1. TEM imaging

Fig. 1 shows a bright field TEM image of an unstained section of the pulverized toner. The roughly ovoid shape that is about 5 μm in the image corresponds to the toner particle. The magnified image shows there is no contrast among the component materials except for some carbon black particles with 50 nm diameter in the toner particle. Because the basis for TEM contrast in non-crystalline materials like the

---

[1] aXis2000 is written in interactive data language (IDL). It is available free for non-commercial use from http://unicorn.mcmaster.ca/aXis2000.html.
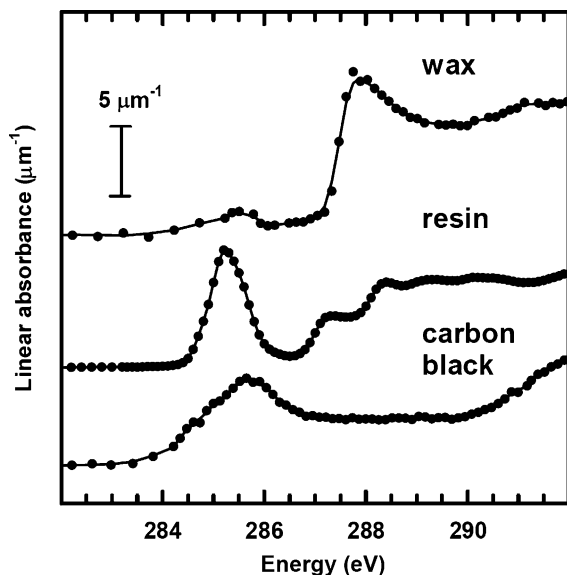
Fig. 3. Reference C 1s spectra of wax, toner resin and carbon black placed on an absolute linear absorbance scale, the solid line is a guide to the eye, from a 3-point smooth of the data.

organic compounds in toner is the difference of the elastic scattering intensity of the incident electron (Nagata, 1993), which in turn is mainly related to differences in the density/thickness of materials, the carbon black particles, which have higher density than the resin, are readily observed in toners. On the other hand wax and resin have about the same density, and thus, they cannot be easily distinguished by TEM. Fig. 2 shows TEM images of a section stained by RuO_4. White contrast can be observed on the right hand side of the toner particle and at the center in the magnified image. Because the straight chain hydrocarbons in wax are relativity inert to reaction with RuO_4 (Trent et al., 1983), the wax presents more white contrast than the resin in the toner. Therefore, it is possible to observe the wax in the toner by staining. Though the carbon black particles are involved in this toner, they cannot be seen in Fig. 2, since the resin stained by RuO_4 is darker than the carbon black particles.

3.2. STXM spectroscopy and chemical component maps

The C 1s NEXAFS spectra of the toner resin, wax and carbon black are shown in Fig. 3. The spectra, originally recorded in transmission mode from pure materials, have been converted to absorbtion (Beer–Lambert Law) and then placed on an absolute linear absorption scale by matching the signal below 280 eV and above 320 eV (extended range spectra are not shown) to the response expected for a material with the known elemental composition and density of each component, based on weighted sums of tabulated X-ray absorption coefficients of the elements (Henke et al., 1993).
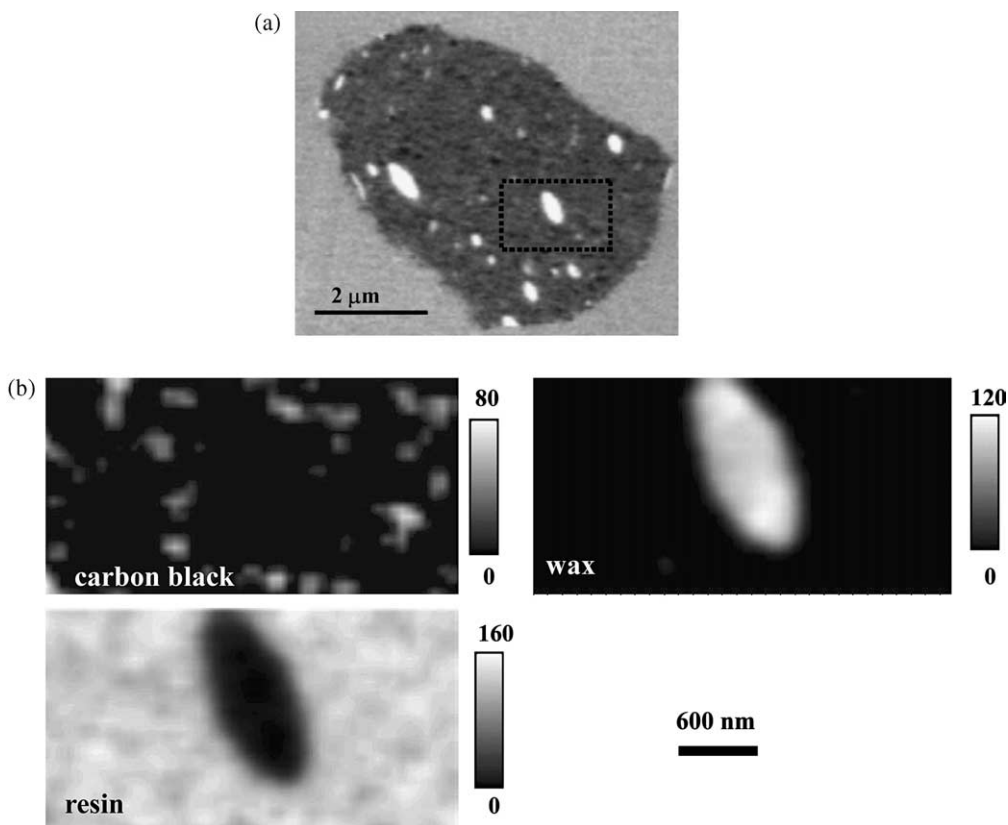

Fig. 4. (a) STXM transmission image at 285 eV of a section of a whole toner particle (b) chemical component maps of part of (a) indicated by dotted line, derived from SVD of a C 1s image sequence. The grayscale indicates thickness in nanometer.

In the 282–292 eV region these spectra are very different, providing the basis for high contrast differentiation of the chemical components. The spectrum of the resin has a sharp, high intensity peak at 285 eV corresponding to the C 1s→ $\pi^*_{C=C}$ transition at the phenyl rings of the aromatic resin species, that of carbon black shows a much broader π^* peak stretching from 284 to 286 eV, which is associated with a broad range of graphitic environments in the 50 nm particles, while that of the aliphatic wax has a very weak peak at 285 eV (which may be associated with a small amount of radiation damage) but instead, shows a strong, broad peak at 287.7 eV associated with C 1s→C–H transitions. All three species have more complex spectral structure above 290 eV, which is associated with a range of transitions to the various types of σ^* orbitals in each species. While the shape at higher energy can assist in chemical identification, the range from 282 to 292 eV was found to be best for differentiating the majority species in toners by STXM image sequences.

Fig. 4(a) shows the STXM transmission image at 285 eV of a section of a toner. At this energy the resin absorbs strongly, the carbon black particles relatively weakly, and the wax has negligible absorption. Fig. 4(b) presents quantitative maps of the carbon black, wax and resin components in the area surrounded by the dotted line in Fig. 4(a). These component maps were obtained by SVD analysis of a sequence of 40 images between 282 and 292 eV, using the energies specified in the experimental section. Comparing the STXM transmission image with the component maps, the round shape with white contrast in the image corresponds to the wax component. Fig. 4(b) shows that the carbon black particles are included in the resin but not in the wax. Therefore, STXM provides simultaneous observation of spatial distributions of wax, resin and carbon black in toners.

3.3. Chemical information about the wax from STXM

A more detailed examination of the spectral contrast in the region of the wax particle in the chemical component map (Fig. 4(b)) shows that it does not have uniform contrast in the optical density image at 287.7 eV shown in Fig. 5(a). In particular, there is a difference in contrast between the upper and lower regions of the wax. C 1s spectra, extracted from the upper and lower side of the wax particle (shown as white regions in Fig. 5(b)), are presented in Fig. 5(c). One sees that, although the general shape is similar, there is a considerable difference in the intensity of the peak at 287.7 eV between the two ends of the wax particle. Fig. 5(d) shows the chemical component maps of the different wax species derived by using these spectra as the reference. The wax is divided into two regions with spatial distributions that reflect the contrast
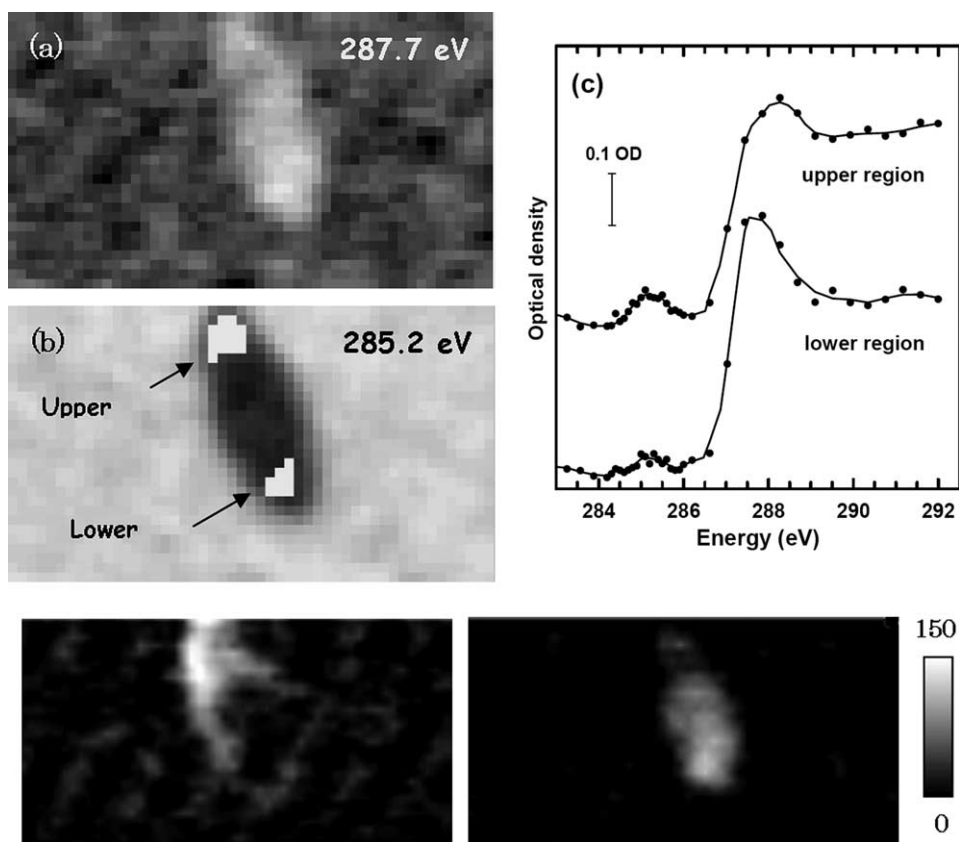

Fig. 5. (a) Optical density image at 287.7 eV, (b) OD image at 285.2 eV with superimposed region identification. (c) C 1s spectra extracted from the upper and lower regions in the wax, corresponding to the pixels highlighted in white in (b). (d) Chemical component maps derived by using the spectra of Fig. 5(c), along with those of wax, and carbon black, as the reference.

variation in the optical density image at 287.7 eV (Fig. 5(a)). What is the origin of this difference in the two components? One possibility is differences in degree of crystallinity and/or molecular orientation since it is known from studies of polyethylene and short chain alkanes (Scholl et al., 2003; Ade et al., 2004) that the C–H transition at 287.7 eV is quite strongly affected by degree of crystallinity and direction of

the chain orientation. This differentiation of wax subcomponents illustrates the power of STXM to provide chemical information about wax in toners beyond the basic level of quantitative mapping of majority components.

3.3.1. Chemical information about the resin from STXM

Comparing the chemical component map for the wax (Fig. 4(b)) with individual images in the sequence brought
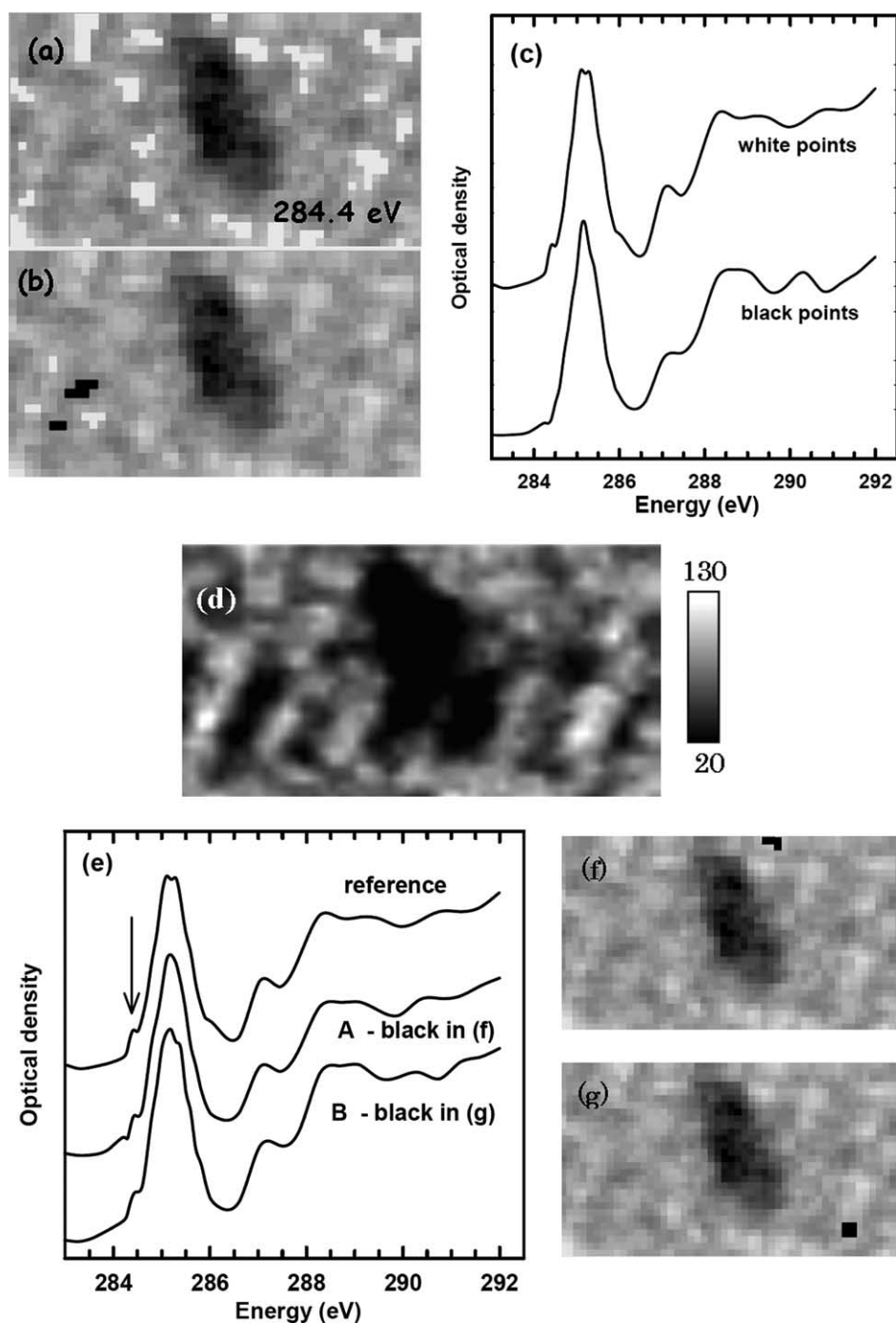

Fig. 6. (a) Optical density image at 284.4 eV. White regions correspond to carbon black particles. (b) is the same image as (a) except for white and black points on left hand side. (c) The spectra extracted from the brighter (white points in Fig. 6(b)) and darker (black points in Fig. 6(b)) regions. (d) Map of the bright resin component derived by using the spectra of Fig. 6(c), along with those of wax, and carbon black as the reference. (e) Spectra extracted from the black points indicated in (f) and (g). All spectra have a shoulder at 284.4 eV, indicated by the arrow.

additional chemical information about the wax. When we examine the resin map in comparison to that of individual images, we find that there is bright and dark contrast in the resin in the optical density image at 284.4 eV (Fig. 6(a)), indicating non-uniformity in the chemistry of the resin. The spectra of lighter and darker contrast regions in the 284.4 eV image are plotted in Fig. 6(c), with the regions from which these spectra are extracted being indicated by white points (brighter contrast regions) and by black points (darker contrast regions) in Fig. 6(b). These points were selected from the lower left hand side of the region examined to avoid possible contamination from the spectrum of any carbon black particles. There is a small but distinct and reproducible difference in the intensity of the shoulder at 284.4 eV in the C 1s spectra of the brighter and darker regions of resin. Fig. 6(d) shows one of the chemical component maps of the resin components derived by SVD analysis using the spectra plotted in Fig. 6(c) as the reference. Though the bright resin map shows a very complicated dispersion, it looks like the optical density image at 284.4 eV. Fig. 6(e) presents the spectra extracted from two points in the bright resin map to validate the analysis. The shoulder at 284.4 eV is recognized clearly in all spectra. Based on this more detailed investigation of the resin signal, it is clear that STXM also provides chemical information on resin chemistry and dispersion in toners.

4. Summary

By comparison of images with and without staining, TEM can highlight the spatial distribution of either carbon black or wax relative to the resin. However, this is not ideal if the goal is a detailed and simultaneous investigation of all components. Although a much lower spatial resolution microscopy ($\sim$50 nm in this work, versus $<$1 nm for TEM), STXM not only provides simultaneous observation of the spatial distributions of wax, resin and carbon black in toners, but it also provides detailed chemical information about the wax and the resin components and their micro environment. The strength of the STXM technique is the strong functional group, local bonding and orientation sensitivity of NEXAFS spectroscopy, which can reveal extensive chemical information at high spatial resolution using multiple energy image sequences. Observation with STXM is a very useful tool for toner development since it provides detailed, quantitative chemical information about dispersion and chemical state of the organic materials in toner particles.

Acknowledgements

References

Ade, H., 1998. In: Samson, J.A.R., Ederer, D.L. (Eds.), X-ray Spectro-microscopy The Physical Sciences, vol. 32. Academic, New York, p. 225.

Ade, H., Urquhart, S.G., 2002. NEXAFS spectroscopy and microscopy of natural and synthetic polymers. In: Sham, T.K. (Ed.), Chemical Applications of Synchrotron Radiation. World Scientific Publishing, Singapore, pp. 285–355.

Ade, H., Zou, Y., Kilcoyne, A.D.L., Wang, Y., Rafailovich, M., Sokolov, J., 2004. X-ray linear dichroism microscopy of short chain alkanes and semi-crystalline polyethylene thin films. Microsc. Microannal. 10 (Suppl. 2), 1020–1021.

Henke, B.L., Gullikson, E.M., Davis, J.C., 1993. Low energy X-ray Interaction Coefficients At. Data Nucl. Data Tables 54, 181–297.

Hitchcock, A.P., 2001. Soft X-ray spectromicroscopy of polymers and bio-polymer interfaces. J. Synchrotron Rad. 8, 66–71.

Hitchcock, A.P., Araki, T., Ikeura-Sekiguchi, H., Iwata, I.N., Tani, K., 2003. 3d chemical mapping of toners by serial section scanning transmission X-ray microscopy. J. Phys. IV France 104, 509–512.

Hitchcock, A.P., Morin, C., Zhang, X., Araki, T., Dynes, J.J., Stover, H., Brash, J.L., Lawrence, J.R., Leppard, G.G., 2005. Soft X-ray spectro-microscopy of biological and synthetic polymer systems. J. Electron Spectrosc. Rel. Phen. 144-147, 259–269.

Itoh, Y., Kishida, H., 2003. Specimen preparation and microscopy of toner sections. J. Electron Microsc. 43, 42–44.

Kiatkamjomwong, S., Pomsanam, P., 2003. Synthesis and characterization of styrenic-based polymerized toner and its composite for electro-photographic printing. J. Appl. Polym. Sci. 89, 238–248.

Kilcoyne, A.L.D., Steele, W.F., Fakra, S., Hitchcock, P., Franck, K., Anderson, E., Harteneck, B., Rightor, E.G., Mitchell, G.E., Hitchcock, A.P., Yang, L., Warwick, T., Ade, H., 2003. Interferometrically controlled scanning transmission microscopes at the Advanced Light Source. J. Synchrotron Rad. 10, 125–136.

Koprinarov, I.N., Hitchcock, A.P., McCrory, C.T., Childs, R.F., 2002. Quantitative mapping of structured polymeric systems using singular value decomposition analysis of soft X-ray images. J. Phys. Chem. B 106, 5358–5364.

Nagata, F., 1993. Developments in applications of high voltage electron microscope. J. Electron Microsc. 42, 371–377.

Scholl, A., Fink, R., Umbach, E., Mitchell, G.E., Urquhart, S.G., Ade, H., 2003. Towards a detailed understanding of the NEXAFS spectra of bulk polyethylene copolymers and related alkanes. Chem. Phys. Lett. 370, 834–841.

Stöhr, J., 1991. NEXAFS Spectroscopy. Springer Tracts Surface Sci., 25.

Trent, J.S., Scheinbeim, J.I., Couchman, P.R., 1983. Ruthenium tetraoxide staining of polymers for electron microscopy. Macromolecules 16, 589–598.

Warwick, T., Ade, H., Kilcoyne, A.L.D., Kritscher, M., Tyliszczak, T., Fakra, S., Hitchcock, A.P., Hitchcock, P., Padmore, H.A., 2002. A new bend magnet beam line for scanning transmission X-ray microscopy at the advanced light source. J. Synchrotron Radiat. 9, 254–257.